Med Biol Eng Comput
DOI 10.1007/s11517-011-0802-7

ORIGINAL ARTICLE

A pilot study of a phenomenological model of adipogenesis in maturing adipocytes using Cahn–Hilliard theory

F. J. Vermolen · A. Segal · A. Gefen

Received: 7 February 2011 / Accepted: 2 July 2011

Abstract We consider the accumulation and formation of lipid droplets in an adipocyte cell. The process incorporates adipose nucleation (adipogenesis) and growth. At later stages, there will be merging of droplets and growth of larger droplets at the expense of the smaller droplets, which will essentially undergo lipolysis. The process is modeled by the use of the Cahn–Hilliard equation, which is mass-conserving and allows the formation of secondary phases in the context of spinodal decomposition. The volume of fluid (VOF) method is used to determine the total area that is occupied by the lipids in a given cross section. Further, we present an algorithm, applicable to all kinds of grids (structured or unstructured) in two spatial dimensions, to count the number of lipid droplets and the portion of the domain of computation that is occupied by the lipid droplets as a function of time during the process. The results are preliminary and are validated from a qualitative point using experiments carried out on cell cultures. It turns out that the Cahn–Hilliard theory can model many of the features during adipogenesis qualitatively.

keywords Adipose · Adipogenesis · Spinodal decomposition · Finite-element method

F. J. Vermolen (✉) · A. Segal
Delft Institute of Applied Mathematics,
Delft University of Technology, Delft, The Netherlands
e-mail: f.j.vermolen@tudelft.nl

A. Gefen
Department of Biomedical Engineering,
Tel Aviv University, Tel Aviv, Israel

1 Introduction

Wounds, trauma, diet, or tumor resection may cause loss of subcutaneous fat. This raises concerns from an aesthetical point of view and therefore, it is attractive to apply lipoplasty to implant autologous fat. However, the results from this procedure on the longer term, seem to be sub-optimal due to insufficient vascularity, which makes the tissue deteriorate. Despite injection of vascular endothelial growth factor (VEGF) would likely have systematic effects, adipose tissue engineering is currently investigated as a clinical alternative.

Mathematical results about existence, uniqueness, stability of the solution to Cahn–Hilliard equations were described in studies due to [2, 8, 33], to mention a few. The Cahn–Hilliard equations describe microstructural changes involving nucleation (in our case adipogenesis), growth, coarsening, merging and dissolution of particles or droplets of varied shape. The phases may co-exist or compete with each other. As an alternative to diffuse interface models, such as the Cahn–Hilliard equation, it is possible to use the so-called sharp interface models. In these models, the interface between adjacent phases is sharp, in the sense that it involves a discontinuity of the (derivative of the) solution. The interface is tracked explicitly by means of moving mesh method [7, 22, 31] or a level-set method [6, 14, 15, 28]. Classical Stefan problems fall within the class of sharp interface models. The diffuse interface models, such as the Cahn–Hilliard equation, also track the content of a chemical by diffusion and involve a smooth solution with a rapid change over the interfacial region, which separates the adjacent phases. From a numerical point of view, the interfacial region has to be discretized with a sufficiently high resolution. Often, one employs mesh adaptive methods to have a sufficiently high resolution in the interface

Published online: 15 July 2011

region and a small resolution away from the interface where the resolution does not need to be that high. The diffuse-interface models are, opposed to the sharp interface models, capable of dealing with the appearance of new particles or lipid droplets. A final class of Lifschitz–Slyozov–Wagner (LSW) models tracks the statistical size distribution of the nucleating particles or lipid droplets. An example is described by Myhr and Grong [23].

Besides the applications and scientific fields that were mentioned until now, there is a growing interest in Cahn–Hilliard equations in the community of mathematical biology. The reason is that separation phenomena play an important role in this scientific field. Wise et al. [37] recently presented a multi-species Cahn–Hilliard problem extended with advection with an application of modeling nonlinear growth of tumors. The same phenomenon is modeled using a sharp interface model by Macklin and Lowengrub [20]. There is a reasonable qualitative agreement between both approaches. Further, examples of Cahn–Hilliard applications in the field of biomaterials are described in Seitz et al. [32] and Fan et al. [10].

In this study, we show by numerical experiments compared to adipocyte cell culture experiments that the Cahn–Hilliard equation gives the right phenomenological picture. It is not yet the aim of this study to describe adipogenesis quantitatively, nor will all biological issues such as the penetration of triglycerides into the adipose cell be modeled. The expansion of the volume of an adipose cell due to adipogenesis is not taken into account in this study. Nevertheless, it is the first study to model accumulation of lipid droplets in adipocytes which is critically needed for supporting adipose tissue engineering, even if the description is merely phenomenological. The experimental results that we use for a qualitative comparison were presented in more detail by Or-Tzadikario [27].

We stress that this article does not aim at being very mathematical. For more mathematical and numerical issues, we refer to [35] and references therein. The important innovation in this study concerns the application of Cahn–Hilliard equations to phenomenologically model apidogenesis and to compute the lipid droplet fraction and number of lipid droplets for arbitrary meshes in two spatial dimensions. We also note that a huge variety of simulations using the Cahn–Hilliard equation can be found in literature.

2 Methods

2.1 Cahn–Hilliard theory

We present some issues from the Cahn–Hilliard theory. As an alternative model that tracks several issues concerning adipose genesis, we briefly mention the LSW model, which is formulated to provide tracking the statistical lipid droplet size distribution, rather than the individual droplets.

The mathematical concepts of the Cahn–Hilliard equation are described as follows. Let Ω be the bounded domain of computation over which the solution of the Cahn–Hilliard equation is determined. Let Ω be bounded by $\partial\Omega$. One can think of Ω as a section within an adipose cell. Let c be the volume fraction of the triglycerides phase in the binary system, i.e., a system that consists of two species only, then, the total Ginzburg–Landau free energy of the system is given by [5, 19, 21, 37]

$$F(c) = \int_{\Omega} \left\{ f(c) + \frac{\kappa}{2} |\nabla c|^2 \right\} \mathrm{d}V, \tag{1}$$

where κ denotes the gradient energy coefficient. This Ginzburg–Landau free energy expression is also treated as a Lyapunov functional, which is used to answer stability, existence and uniqueness questions. Further, $f(c)$ is the bulk free energy, which can be obtained from thermodynamic databases. A typical form is the following

$$f(c) = RT\left(\frac{c\ln(c)}{N_1} + \frac{(1-c)\ln(1-c)}{N_2}\right) + \omega c(1-c). \tag{2}$$

Here ω denotes the interaction parameter. An example of a bulk free energy of the above form is shown in Fig. 1. Here N_1 and N_2 are related to the molecular size. The values c_{L} and c_{R} are known as the binodal points, determined by the common tangent construction, as shown in Fig. 1. The second term in Eq. 1 is crucial in the interfacial region, where the gradient of c is large. Therefore, the second term is also referred to as the interfacial energy. In our application, we assume that triglycerides appear in solution to such a high extent that, after possible chemical reactions, the initial condition resides between the spinodal values in Fig. 1, which is in the miscibility gap, given by the region in Fig. 1 where $f''(c) < 0$. This gives a meta-stable mixture, in other words a super-saturated solution, and then as a result of small spatial fluctuations, the triglycerides will oil out resulting into the segregation of lipid droplets. These lipid droplets contain a high concentration of triglycerides, which are typically near the higher bimodal value for triglycerides. Hence, we have two phases: the highly concentrated lipid droplets and the dilute concentrated part of the cytosol. Since, the overall energy is lower for this latter decomposed state, it follows that the decomposed state is more stable. The Cahn–Hilliard is used to model the kinetics of the transition from the initial state to the end state. The kinetics of the aforegoing chemical reactions to be so fast so that they are assumed not to determine the overal kinetics of adipogenesis. We consider a situation in which all triglycerides have been distributed equally over all cells, except for small random perturbations. We

assume that the total mass of triglycerides is conserved. Furthermore, we assume that convective processes within the cytosol are negligible, and that the only mechanism for transport is nonlinear diffusion. These aspects are dealt with when solving the Cahn–Hilliard equation, whereas the Allen–Cahn equation is contained in a phase field model with nonconserved variables. The Cahn–Hilliard equation can be seen as a modified nonlinear diffusion equation in which uphill diffusion occurs if the concentration resides between the spinodal values, see Fig. 1. The Cahn–Hilliard equation is capable of modeling lipid droplet formation from small perturbations around the initial meta-stable state, growth, and Oswald ripening, which is the growth of larger lipid droplets at the expense of the shrinking small lipid droplets. All these phenemona occur in the experimental data. In this model, we do not incorporate the kinetics of formation of triglycerides. As, we only focus on the actual lipid droplet formation, growth, and fusion. In future studies, we want to consider these issues in more detail. We note that this study is preliminary, in which we show our first plans of attack.

The diffusive flux, J, is postulated to be proportional to the gradient of the chemical potential, see for instance [19, 21], hence

$$J = -M\nabla\mu(c) = -M\nabla\frac{\delta F(c)}{\delta c}. \tag{3}$$

Here the variational derivative $\frac{\delta F(c)}{\delta c}$ is given by

$$\frac{\delta F}{\delta c} = f'(c) - \kappa\Delta c. \tag{4}$$

Furthermore, M denotes the mobility, which is treated as a constant by most authors, and Δc represents the Laplace Operator on c, but Elliott and Garcke [9] treat the case of a concentration-dependent mobility. The mobility is a measure for the jump rate and rate of motion of the molecules involved. In this study, we will assume M to be a constant. Substitution of Eq. 4 into 3 and use of the mass-balance,

$$\frac{\partial c}{\partial t} = -\nabla\cdot J, \tag{5}$$

gives the Cahn–Hilliard equation on Ω

$$\frac{\partial c}{\partial t} = \nabla\cdot\{M[f''(c)\nabla c - \kappa\nabla\Delta c]\}. \tag{6}$$

In the above equation, the second derivative $Mf''(c)$ acts like an adjusted diffusion coefficient with respect to the adipocyte cell's composition. The fourth order term, with κ, in the Cahn–Hilliard equation is also considered as a stabilization term, for the case where $f''(c) < 0$. This equation has been applied to model phase segregation and spinodal decomposition in numerous studies [1, 9, 16, 19, 21, 34], in which the list is far from complete. In the case of phase-separation and spinodal decomposition, the second derivative of f with respect to c becomes negative in the interface part of the domain. Physically, the negative values of the second derivative of f give rise to "uphill diffusion", which is diffusion from low concentration areas to high concentration regions. As boundary conditions we use symmetry conditions, i.e.,

$$\frac{\partial c}{\partial n} = \frac{\partial(\Delta c)}{\partial n} = 0, \quad \text{on } \partial\Omega. \tag{7}$$

These two boundary conditions on each point of boundary $\partial\Omega$ and an initial condition are necessary and sufficient for a uniquely defined solution. In many other studies, periodic boundary conditions are used instead. Further, we have an initial condition for the concentration c:

$$c = c_0, \quad \text{for } t = 0. \tag{8}$$

It should be realized that $\sqrt{\kappa}$ is a measure of the interface thickness. Furthermore, one can demonstrate that solutions to the Cahn–Hilliard equation, with our boundary conditions, satisfy the following fundamental properties:

1. Solutions to the Cahn–Hilliard equation are mass conserving, hence with the current boundary conditions, it follows that $\frac{\mathrm{d}}{\mathrm{d}t}\int_\Omega c\mathrm{d}\Omega = 0$;
2. The total energy is non-increasing, that is $\frac{\mathrm{dF(c)}}{\mathrm{d}t} \leq 0$.

In our present model, we use the Cahn–Hilliard equation to model adipogenesis, which is the nucleation, growth and merging of lipid droplets in maturing and mature adipocytes. The cytoplasm is assumed to be in the lipid droplet phase if the solution exceeds a certain threshold. To be more explicit, this amounts to the following portion of Ω :

$$\Omega_\mathrm{L} = \Omega_\mathrm{L}(t) = \{\mathbf{x}\in\Omega : c(\mathbf{x},t) \geq \hat{c}\}, \tag{9}$$

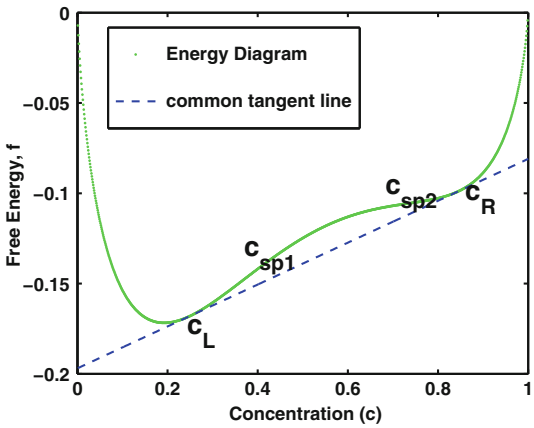

Fig. 1 A plot of a Gibbs free energy function and the determination of the binodal concentrations

where Ω_L denotes the region that is occupied by the lipid droplets. What we are after is:

1. The number of lipid droplets as a function of time;
2. The lipid area per cross section as a function of time, that is $\frac{|\Omega L(t)|}{|\Omega|}$, in which $|\Omega_L(t)|$ and $|\Omega|$, respectively, denote the areas of the regions Ω_L and Ω.

In [12], the time behavior of the total energy has been evaluated and it is found that the total energy decays via a $t^{-\frac{1}{4}}$-law at early stages and that this behavior changes to a $t^{\frac{1}{3}}$-decay law at the coarsening stages. This is in line with the Mullins–Sekerka problem. Here, the lipid droplets circumference is minimized under a constant lipid droplet area in two spatial dimensions.

In the alternative model due to Lifshitz, Slyozov, and Wagner, nucleation and early growth are considered as the only processes in adipogenesis. The model keeps track of the statistical distribution of the lipid droplets, in which it is assumed that all droplets are spherical. A combination of the statistical distribution of the droplet radius and the rate at which the radius changes gives the mean droplet radius and the volume fraction. This model does not incorporate phenomena over large times and deviation from spherical geometry. Therefore, we do not further elaborate on this type of models. An excellent article on this topic has been written by [25].

2.2 Numerical procedure

2.2.1 *The Cahn–Hilliard equation*

To solve the Cahn–Hilliard equation, we use a standard Galerkin finite-element method with order reduction, that is the Cahn–Hilliard equation is split into a system of partial differential equations with only second-order spatial derivatives. This is done to avoid the necessity of the use of higher order elements with stronger requirements for continuity (for instance in $\mathbb{R}^1$, it can be demonstrated easily that elements need continuity up to at least the first order spatial derivative, and hence for instance cubic Hermitian elements or continuous quadratic elements are used). The domain of computation is divided into triangles and the element basis functions that we use are linear over each element. We use an implicit Euler time integration method, where we use a Picard method to solve the obtained nonlinear algebraic system of equations at each timestep. The algorithm has been implemented both for 2D and 3D geometries, in which tetrahedra are used in 3D geometries. The method that we used has been described in [35], where also a score of alternative methods are presented with respect to time integration and the mentioning of spectral and discontinuous Galerkin methods.

2.2.2 *The determination of the number of droplets and droplet area*

As a post-processing step, we need to compute the area that is occupied by the lipid droplets in a given cross section as a function of time. If the solution at a certain time, t and location, $\mathbf{x}$, exceeds a certain threshold, that is $c(\mathbf{x}, t) \geq \hat{c}$, then the location is assumed to be occupied by the lipid droplet at this time t. The total area that is occupied by the lipid droplets in a given cross section is determined by a volume of fluid method, which is also explained in this section. The postprocessing algorithm has been implemented for 2D-configurations up to now.

Counting the lipid droplets

The droplets are defined via the relation $c > \hat{c}$, where $\hat{c}$ is a given threshold value. The solution, c, is known in all nodal points and since we use linear triangular elements, the solution, c, varies linearly over each element at a certain time t. To find the lipid droplets in terms of its number and area, we proceed as follows:

Marking of the nodes

First, all nodes are for which $c > \hat{c}$ are marked with a value of 1. Nodes for which $c < \hat{c}$, are marked with -1 and all other nodes are marked with 0.

Marking of the elements that do not belong to the droplets

Next, all elements in the domain of computation are marked with 0. The elements of which all vertices give $c < \hat{c}$, are marked with -1. Hence, for example at a certain time, we could have Given element e with vertices $\{1, 2, 3\}$, then

$$e_{\text{mark}}(e) = \begin{cases} -1, & \text{if } c_i < \hat{c}, \quad \text{for all } i \in \{1,2,3\}, \\ 0, & \text{else .} \end{cases} \tag{10}$$

Herewith, all elements that do not belong to any droplet have been marked with a value of -1. All the other elements belong a droplet. Next, we have to figure out to which droplet each of these elements belong.

Marking the elements corresponding to the first droplet

We examine the marking value of all the elements and the first element with a mark 0 is marked to a value 1 to indicate that it belongs to droplet 1. Subsequently, all neighbors of this element that have a mark 0 are marked to 1. Then, all neighbors, with mark 0, of the aforementioned elements that were just marked with a value of 1, are marked to a value 1 as well. This is repeated for all neighbors with mark 0, until no neighbors with mark 0 are found anymore. Now, all elements that correspond to droplet 1 have been found, and the area of droplet 1 can be computed (see the next subsection). The set of all elements that belong to a certain droplet is referred to as *the active set* of this droplet.

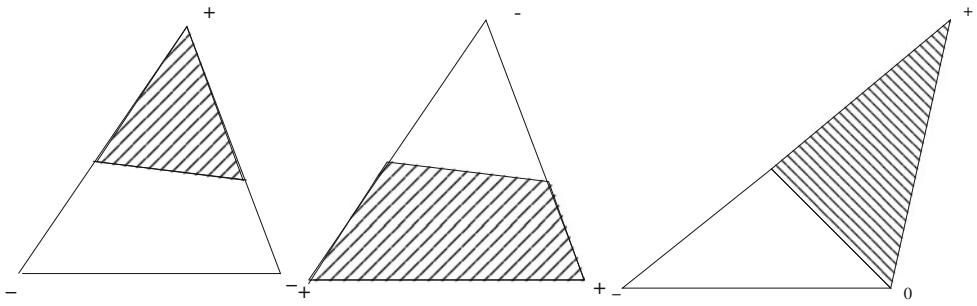

Fig. 2 From *left to right*: two nodes negative − two nodes positive − one node zero

Marking the elements corresponding to all other droplets

If there are still any elements with mark 0, then the sequence number of the droplet is incremented (increased by one). This sequence number indicates which droplet we are working on. The aforementioned process in the previous paragraph is repeated with the first found element with mark 0.

The process is repeated under incrementing the sequence number of the droplet until all elements are marked with a value that is different from 0, being -1 if this element does not belong to any droplet (that is $c < \hat{c}$ for all its vertices), or else being the sequence number of the droplet the element belongs to. We summarize this in the following algorithm:

Algorithm 1:
Mark all nodes with -1, 0 or 1, depending on their value.
Mark all elements with 0, except these with all nodes $< \hat{c}$ get -1.
seq_droplet := 0
while there are still elements marked zero **do**
  seq_droplet := seq_droplet+1
  Find first element that is marked zero and add to active set
  while there are still elements in the active set **do**
    element := last element in active set
    mark element with seq_droplet
    add all zero marked neighbors of element to active set
  end while
end while

Here, as mentioned earlier, the active set corresponding to droplet i represents the set of all elements that belong to droplet i. In this way, all elements are marked -1 or positive indicating to which droplet they belong. In this way, each individual lipid droplet is tracked and also its area occupied in a given cross section can be evaluated in the course of time.

The computation of the area occupied in a given cross section by the lipid droplets

During the marking of the elements, we paint the part of the element belonging to the droplet with a color and also compute the area of this part. This area is added to the total area of the droplet. For this process, we need to distinguish between three situations.

The most simple one is the case in which all three nodes are marked with 0 or 1. In that case, the whole element should be painted and the area is exactly the area of the triangle. If not all three nodes are marked with 0 or 1, then linear interpolation is used to determine the points on the sides of the triangular elements for which $c = \hat{c}$.

When two nodes are marked negative, we have the situation of Fig. 2. The dashed region corresponds to the droplet and the area of this small triangle can be computed in the same way as that of the large triangle.

If two nodes are marked positive and one negative, we get the situation of Fig. 2. In this case, the dashed region is a quadrilateral. The easiest way to compute the area is to subtract the area of the small triangle from the large one.

Finally, we have the situation where one of the nodes coincides with the boundary of the droplet, and the other two are inside and outside the droplet. This situation is sketched in Fig. 2.

Note that the solution is linear over each element. Since, the procedure to get the lipid droplet area in an element is based on linear interpolation and on exact computation of the area, the current procedure will not give any contribution to the numerical error.

3 Results

We emphasize that an abundance of simulations with the Cahn–Hilliard equation is available. So, the presented contours of the solution to the Cahn–Hilliard equation are not original. Though, the qualitative comparison with the experiments on lipid droplet formation as well the application of the lipid droplet count and area determination (and applicability to arbitrary meshes) are original. As an example of the numerical solution of the Cahn–Hilliard equation, we consider a simple square domain $\Omega = (0, 1)^2$. Further, the initial condition of this simplified adipocyte cell is chosen by

$$c_0(x_i, y_i) = 0.5 + 0.001 \cdot \text{rand}(1), \tag{11}$$

at each gridpoint i with location (x_i, y_i). This condition reflects the assumption that initially the adipose cell

consists (apart from its nucleus) of a perfect mixture with a small perturbation. This perturbation is necessary, since each constant initial state will have this constant state as the solution to the Cahn–Hilliard equation with our boundary conditions. In other words, if the solution is initially constant then the solution will not change in time. Further, the function rand(1) is used to generate a random number between 0 and 1 at each gridnode. Further, we use $f''(c) = \frac{c}{1.3} + \frac{1-c}{0.8} - 4.6c(1-c)$, $M = 1$, $\hat{c} = 0.6$, and $\kappa = 10^{-4}$. Homogeneous natural boundary conditions apply at the boundary of Ω. The interfacial width is proportional to $\sqrt{\kappa}$. Further, the initial configuration (11) is unstable since $f''(0.5) < 0$ and hence perturbations start to grow and lipid droplets start to appear. One can see the merging of neighboring droplets, and growth of large droplets at the expense of small droplets, which undergo lipolysis. Figure 3 displays some results at consecutive times. Here, the lipid droplets even merged more, hence the number of droplets decreases, however their total occupied area increases. The number of droplets per area of view is shown in Fig. 4. The behavior of the number of droplets is determined by adipogenesis (nucleation), merging, and growth of larger droplets at the expense of the catabolization (that is, they chemically break down) of small-sized

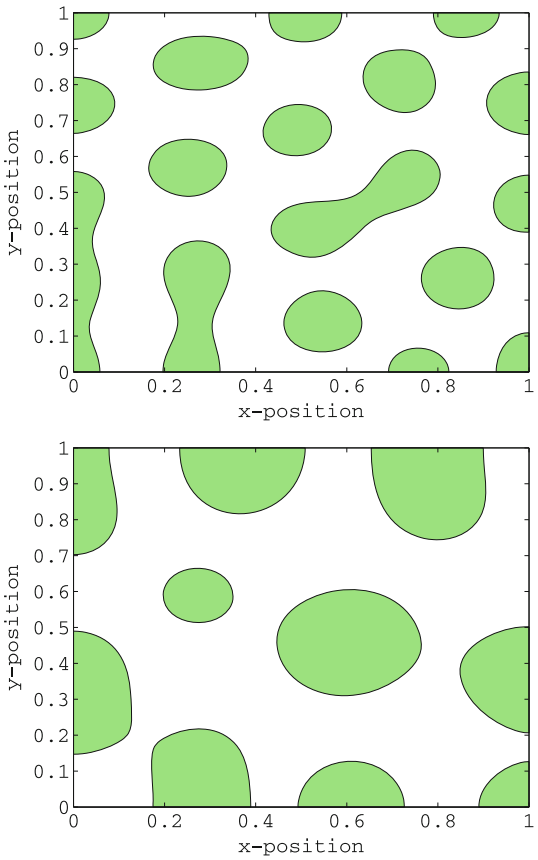

Fig. 3 A plot of the droplets at a dimensionless times $t = 0.25$ and 1

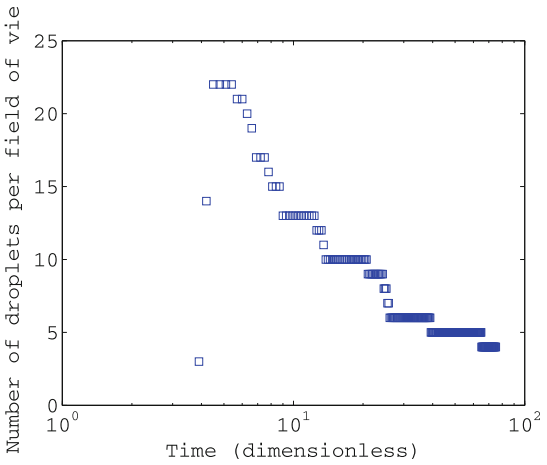

Fig. 4 A plot of the number of lipid droplets per field of view as a function of time, here $\hat{c} = 0.7$

droplets. In Fig. 5, we show the lipid area fraction per field of view as a function of time. From Fig. 4, it can be seen that first there is an incubation time, followed by a sharp increase of the lipid area fraction. This incubation time follows from the fact that the perturbations of the initial state first have to grow until the threshold concentration $\hat{c}$ is reached. Then, subsequently nucleation takes place with a vast increase of lipid area. After the nucleation phenomenon, growth, catabolization, and merging takes over, which makes the increase of area less pronounced. Changing parameters like mobility M, gradient energy κ, and threshold concentration determines the rate of the process and the shape of the curve. Furthermore, the equilibria are determined from the constants N_1, N_2, and ω. As another illustration, we show the influence of the mobility, M, to the evolution of the lipid area fraction in Fig. 5. It can be seen clearly that with a decreasing mobility, the incubation time and slope of the curve increase and decrease, respectively.

Changing the threshold concentration $\hat{c}$, gives the results that were displayed in Fig. 5. In this figure, the curves have been shifted to the left so that there is no incubation time. The reason for this is that the experimental results by Or-Tzadikario [27] also reflect the adipogenesis behavior from the time at which the formation of the lipid droplets starts. It can be seen that the behavior qualitatively reflects the experimental curves in Fig. 8 better, if the threshold concentration $\hat{c}$ is chosen large.

3.1 Model validation against adipocyte culture experiments

This mathematical model was qualitatively compared with previously conducted cell culture experiments which were reported in detail by Or-Tzadikario [27]. For completeness

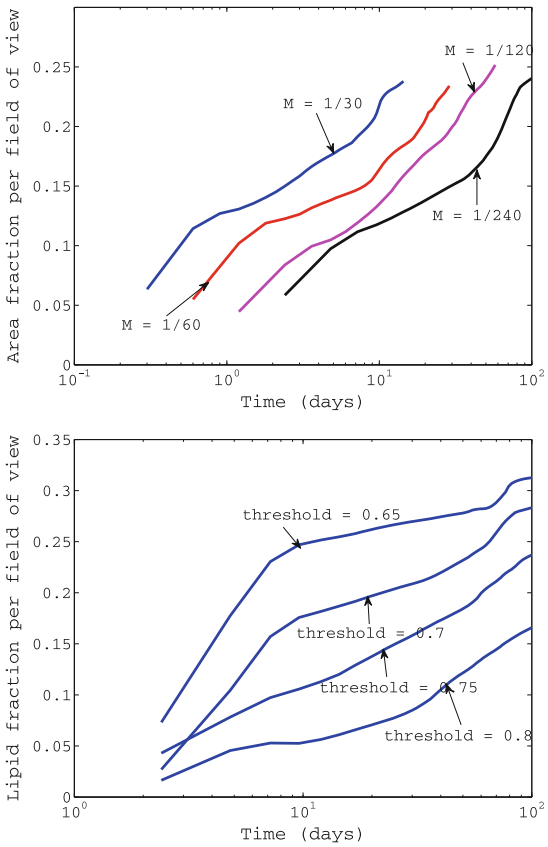

Fig. 5 *Top* A plot of a lipid area fraction per field of view as a function of time for several mobilities. The scale has been chosen logarithmic for the horizontal axis for correspondence to the results in Fig. 8. From the times shown, the incubation times were subtracted, which is in line with Fig. 8, where the measurement started as soon as lipid droplets started to appear. *Top* The threshold concentration was chosen to be $\hat{c} = 0.75$. *Bottom* The mobility was chosen to be $M = 1/240$

and for the purpose of comparisons, we describe these experiments here in brief. Mouse embryo fibroblasts (3T3-L1, passage number 9 or lower) obtained from the American Type Culture Selection (ATCC) were cultured in 75 cm^2 flasks with growth medium consisting of high-glycoses Dulbecco's Modified Eagle Medium (DMEM, 4.5 mg/l; Biological Industries, Israel), 10% fetal bovine serum (Biological Industries), 1% L-Glutamine (Biological Industries), 1% Penicillin–Streptomycin (Pen-Strep; Sigma, Israel), and 0.5% HEPES (Sigma). We allowed cultures to reach maximum confluence of 75–80% before passaging. We induced differentiation in the sufficiently confluent cultures using a differentiation medium that contained the growth medium ingredients plus 5 µg/ml insulin (Sigma), 1 µM dexamethasone (Sigma), and 0.5 µM 3-isobutyl-1-methylxanthine (IBMX;Sigma). Three days later after inducing differentiation (Fig. 6), we changed the medium to a supporting medium that contained the growth medium ingredients supplemented with

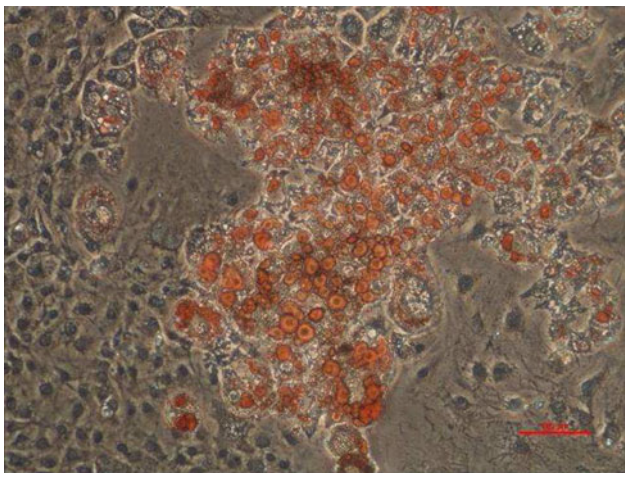

Fig. 6 Lipid droplets developing in 3T3-L1 cell cultures: optical micrograph of a mature adipocyte culture stained with oil red O which selectively stains lipid droplets in the cells in *red* color

5 µg/ml insulin (only). This supporting medium was changed every 2–3 days (Fig. 7).

To monitor the extents and timecourses of accumulation of lipid droplets in the cultures, we developed an image-processing-based method that calculates the percentage area of lipid droplets in a field of view of an optical microscope, as well as numbers and sizes of droplets from conventional optical micrographs taken consecutively during culturing, without the need of staining the cells. The complete image processing algorithm, including the Matlab code in which it was implemented, is provided in Or-Tzadikario [27] and is outside the focus of this article. However, for the purpose of qualitative comparisons of this simulation data against the experimental percentage lipid area per field of view and the number of the lipid droplets in a cell versus the logarithm of time (in days) for 30

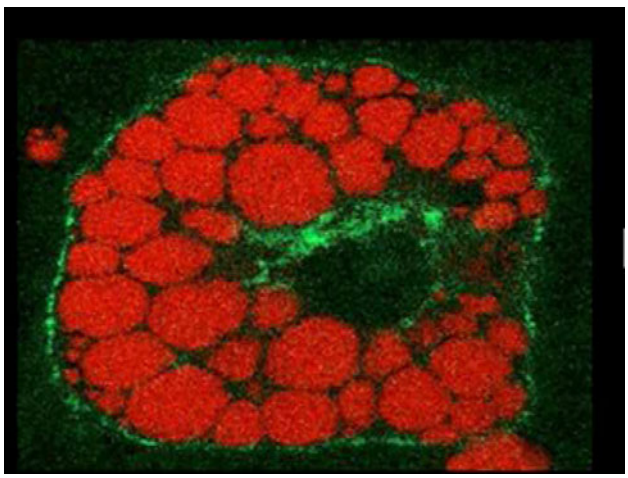

Fig. 7 Lipid droplets developing in 3T3-L1 cell cultures: fluorescent micrograph of a single differentiated adipocyte cell stained with nile-red that demonstrates the lipid droplets contained in the cell

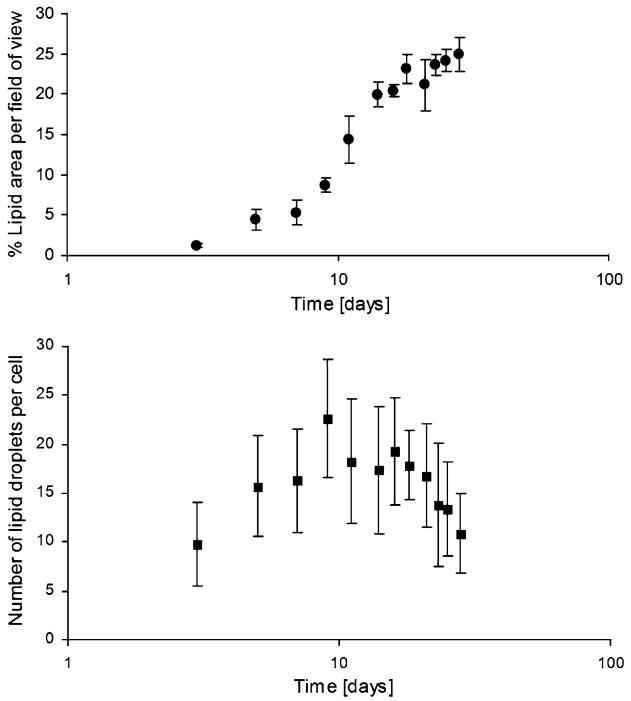

Fig. 8 Experimental results from lipid accumulation studies in 3T3-L1 cell cultures differentiated in media containing 10% fetal bovine serum and 5 μg/ml insulin: *top* percentage lipid area per field of view versus the logarithm of time (in days) from induction of differentiation. *Bottom* number of lipid droplets versus the logarithm of time (in days) from induction of differentiation. These experimental data were adopted from Or-Tzadikario et al. [27]. The number of lipids significantly increases in the nucleation phase—up to experimental day 10—and then significantly decreases due to fusion of adjacent droplets

consecutive culturing days, as obtained from Or-Tzadikario's image processing algorithm (Fig. 8). It is evident that qualitatively, the timecourse of percentage lipid area predicted by the Cahn–Hilliard theory (Fig. 5) very much resembles the experimental data (Fig. 8). Likewise, the experimental data of numbers of lipid droplets in cells (Fig. 8) show that the Cahn–Hilliard theory was able to successfully simulate the timecourse behavior of this outcome measure as well (Fig. 4), particularly the initial increase in lipid droplet during the nucleation phase and the later decrease in their number when adjacent lipid droplets fuse together.

4 Discussion

As pre-adipocyte cells mature from fibroblast-like cells to adipocyte cells, lipid droplets develop, grow, and accumulate (adipogenesis). This process is triggered by the excess of triglycerides. We are aware of the enormous chemical complexity of the process of lipid droplet formation. Boström et al. [3, 4] report that diglycerides (an intermediate product) undergo a diacylglycerol acyltransferase, acting as a catalyst, reaction with acyl-CoA to form triglycerides. The catalytic reaction takes place in the microsomal membranes. The formed triglycerides are highly hydrophobic and hence have a limited solubility in the membrane monolayer. Therefore, the cytosol becomes unstable, and triglycerides start to oil out to form lipid droplets which gradually grow and merge. This process is similar to the process of spinodal decomposition, in which an initially unstable, possibly one phasic, region starts to decompose into two or more phases. Spinodal decomposition as a separation of phases is commonly modeled by the use of diffuse interface models, also called phase-field models, such as the Allen–Cahn or Cahn–Hilliard equations. The Allen–Cahn equations do not conserve mass in general, but are somewhat closer to diffusion equations in the sense that besides the phase, also the content of a chemical is tracked explicitly. The Cahn–Hilliard equation tracks the phase of the configuration. Further, the Cahn–Hilliard equation is a fourth-order partial differential equation in space and first order in time.

The biochemical mechanism by which lipid droplets form is not yet completely understood. However, it is generally thought that new triglycerides, formed either in the plasma membrane or in the endoplasmic reticulum, and which are very hydrophilic and have limited solubility, tend to "oil out" as a separate phase into the cytosol and form the core for formation of new cytosolic lipid droplets. The size of the smallest lipid droplets observed in cells by electron microscopy is about 0.1 μm [26]. Lipid droplets can increase in size by fusion, which is independent of triglyceride biosynthesis. In fact, Boström et al. [4] showed that approximately 15% of all droplets in a maturing adipocyte culture are engaged in fusion events at any given time. Lipid droplets can also be catabolized in a process called lipolysis, during which droplets are being broken into free fatty acids and glycerol that are liberated from the cytosol and then enter the circulation. The anabolic hormone insulin inhibits lipolysis.

The Cahn–Hilliard equation describes spinodal decomposition if the initial condition is unstable with respect to perturbations. If a certain threshold (chosen between the spinodal compositions), $\hat{c}$ is used to identify which phase a certain location is in at some time, then at a certain moment the solution exceeds the threshold value at some regions within Ω, that is $|\Omega_L| > 0$. First, the regions are circular and grow. At this stage, nucleation of droplets, or adipogenesis, is modeled. Subsequently, more and more regions will have a solution that exceeds the threshold, and then several droplets merge. In our simulations, an initial solution was chosen such that it represents an initial unstable

equilibrium point of the partial differential equation with boundary conditions. Since the state, though unstable, is an equilibrium, a small perturbation is necessary to trigger the process of spinodal decomposition.

Alternative models may also be useful, such as sharp interface models, i.e., Stefan problems. Without nucleation, it can be shown that the solutions of the Cahn–Hilliard equation converge to solutions to the Mullins–Sekerka problem under appropriate conditions, see for instance the study by Pego [29]. The problem is that these models can only predict later stages of growth, and nucleation, or adipogenesis, cannot be modeled with these models. Another alternative is the use of the LSW models for the lipid droplet size distribution. Although, the last-mentioned model mimics the appearance of lipid nuclei rather well, in particular at the early stages of adipogenesis, the model cannot predict later stages as shape changes and merging of lipid droplets. This is due to the fact that the model is limited to a single shape. Therefore, we think that diffuse interface models are most suitable in this application since they are able to combine the effects of nucleation, growth, and merging (change of shape and topology), which is also observed in the experimental study by Or-Tzadikario et al. [27].

The mobility parameter M, whose influence on percentage lipid area per field of view predicted by the Cahn–Hilliard theory is demonstrated in Fig. 5, can be adjusted to reproduce (and then to predict) the kinetics of adipogenesis in different experimental conditions. In particular, M can be adjusted to simulate adipogenesis in adipocytes cultures from different sources as well as the influence of culture conditions such as insulin concentration, fetal bovine serum concentration, nature of the substrate for culturing, pH of the medium, oxygen supply, or any form of physical or biochemical stress applied on the cultures. Or-Tzadikario et al. [27] primarily studied the effects of insulin and serum concentrations in the cultures, in cells from a cell line source (3T3-L1) as well as in primary cultures of mesenchymal stem cells differentiated to adipocytes. They found different timecourses of the percentage lipid area per field of view as well as the numbers of lipid droplets, depending on the cell origin and concentration of insulin and serum in the culture media. In the future, we plan to relate the mobility parameter M, and other thermodynamic parameters appearing in the energy functional, to each of these culture conditions based on experimental data, so that it would be possible to provide quantitative, rather than qualitative predictions of the extents and timecourses of lipid accumulation and moreover, to predict the effects of changing the insulin or serum concentrations in the medium on the outcome of accumulated lipids.

Another important parameter for the description of the development of the lipid area fraction is the threshold concentration $\hat{c}$. Lower values of the threshold give a more sudden nucleation rate after the incubation (waiting) period. This can be explained somewhat by considering a linearization around the initial state, c_0. For the linearized Cahn–Hilliard equation (around the average of the initial state c_0), given by

$$\frac{\partial c}{\partial t} = M\left[f''(c_0)\Delta c - \kappa\Delta^2 c\right], \tag{12}$$

it can be seen easily for one spatial dimension that solutions of the form $\exp(\sigma t)\sin(\lambda x)$ can be found with $\sigma > 0$. Let

$$\tau := \frac{1}{\sigma}\ln\left(\frac{\hat{c}}{c_0}\right),$$

then, the width of the portion of the domain for which $c > \hat{c}$, which could be interpreted as the width of a 1D lipid droplet, is estimated by

$$\delta(t) = \begin{cases} 0, & \text{if } t < \tau, \\ \frac{1}{\lambda}\left(\pi - 2\arcsin\left(\frac{\hat{c}}{c_0}\exp(-\sigma t)\right)\right), & \text{if } t \geq \tau. \end{cases} \tag{13}$$

Then, the rate of change is given by

$$\delta'(t) = \begin{cases} 0, & \text{if } t < \tau, \\ \frac{2}{\lambda\sqrt{1-\left(\frac{\hat{c}}{c_0}\exp(-\sigma t)\right)^2}}\frac{\hat{c}}{c_0}\sigma\exp(-\sigma t), & \text{if } t \geq \tau. \end{cases} \tag{14}$$

Note that as $t \to \tau$, δ' gets unbounded, which explains the sharp increase of the area fraction per field of view just after the incubation time. Since, it is well known that solutions to the Cahn–Hilliard equation differ significantly from the linearized version, the deviation from linear behavior increases as the threshold concentration increases. Hence, the evolution of the actual lipide droplet size will be different too. From the Lifshitz–Slyozov theory, it is to be expected that the average lipid droplet radius, $\overline{R}$, will evolve as $\overline{R}(t)^3 = \overline{R}_0^3 + \alpha t$ at the later stages, see for instance Küpper et al. [18], among many others. In the last-mentioned reference, the Cahn–Hilliard equation is considered for the simulation of particle growth in metallic systems.

We note that the Cahn–Hilliard model involves more parameters. An optimal fit between model and experiments could be obtained after the use of regression techniques. In Fig. 8, it can be seen that the experimental curve starts differing from zero after a certain incubation time. As time proceeds, the rate of the increase of the lipid area decreases, which again is followed by a sharper increase of this rate. As the system tends to an equilibrium, the area tends to a limit, which slows down the increase rate of the lipid area. Then, coarsening starts taking place, which can be seen by considering the number of lipid droplets in Fig. 8. A similar behavior is reproduced by the simulation curves

in Figs. 4 and 5. Although, our calculations and the experiments carried out by [27] agree from a qualitative point of view, we think that another interesting possibility, is the incorporation of surface energy effects around the lipid droplets. This would give a slower increase of the area fraction of the lipid droplets at the early post-nucleation growth stages. This effect can be modeled using the Cahn–Larché equations, in which the energy functional is entended with a term from elastic energy and the Cahn–Hilliard equation is coupled with a mechanical balance. We plan to incorporate the mechanical effects in future studies to investigate their influence on the early stages of growth of lipid droplets. The combination of Cahn–Hilliard equations with elasticity is studied in [11], among many other studies carried by Garcke and his team and other authors in the (numerical) mathematical community.

Another important issue is the kinetics of reactions before the separation of phases in the cytosol, given that in the experimental setting, the pre-adipocytes were cultured in flasks containing a high concentration of glucose in the medium (4.5 mg/l), which accelerates the formation of lipid droplets. In a real-world scenario, the rate of adipogenesis depends on the availability of glucose. Glucose consumption by the cells was not accounted for in this modeling, nor did we consider other components in the biochemical chain of reactions leading to adipogenesis; rather, we provided a phenomenological description to the physical outcome of lipid droplet formation. Accompanied with this last-mentioned process, the initial concentration, and hence the driving force for the transformation (that is the mechanism in which the triglycerides oil out of the cytosol) may not be homogeneous if the additions would have to diffuse through the cytosol. This diffusion process takes place simultaneously with the segregation process. Last, but not least, we are comparing a 2D-model to 2D-cross-sections in 3D-samples. With our code, it is possible to solve the Cahn–Hilliard equation in three spatial dimensions, but the algorithm of counting the lipid droplets and computing the lipid droplet fraction, in a generic unstructured mesh, has to be adapted to 3D-simulations. The 3D-simulations, including the lipid droplet counts and volume determination are much more expensive. In future studies, we want to improve on these issues. Although, much of the actual biological mechanism behind adipogenesis remains unclear, the Cahn–Hilliard equation gives the right phenomenological picture in the sense that it models nucleation, growth, shrinkage, and merging of lipid droplets. This issue, and the experimental results, imply that the model needs improvement and to be made more complex in accounting for more physical parameters. This is left for further research. This study should be considered as a pilot in using the Cahn–Hilliard type models for simulating adipogenesis, and as a start to use more complicated models which incorporate more of the relevant physics. Furthermore, developing modeling tools for predicting adipogenesis at a cellular scale contributes to the understanding of adipose function at a tissue scale as well, which then has several implications on characterization of biomechanical, see for instance Gefen [13], Natali et al. [24], and Portnoy et al. [30] and bioelectrical, see for instance Kuhn et al. [17], properties of adipose tissue.

Since, the qualitative agreement between the experiments and simulations from Cahn–Hilliard theory is rather good, we conclude that it is plausible that adipogenesis is a mainly diffusion-controlled mechanism.

References

1. Andersson DM, McFadden GB, Wheeler AA (1998) Diffuse-interface methods in fluid mechanics. Annu Rev Fluid Mech 30:139–145
2. Barrett JW, Blowey JF, Garcke H (1999) Finite element approximation of the Cahn–Hilliard equation with degenerate mobility. SIAM J Numer Anal 37(1):286–318
3. Boström P, Andersson L, Li L, Perkins R, Højlund K, Borén J, Olofsson S-O (2009a) The assembly of lipid droplets and its relation to cellular insulin sensitivity. Biochem Soc Trans 37:981–985
4. Boström P, Rutberg M, Ericsson J, Holmdahl P, Andersson L, Frohman MA, Borén J, Olofsson S-O (2009b) Cytosolic lipid droplets increase in size by microtubule-dependent complex formation. Arter Thromb Vasc Biol 25(9):1945–1951
5. Cahn JW, Hilliard JE (1958) Free energy of a non-uniform system. I: interfacial energy. J Chem Phys 28:258–267
6. Chen S, Merriman B, Osher S, Smereka P (1997) A simple level set method for solving Stefan problems. J Comput Phys 135:8–29
7. Crusius S, Inden G, Knoop U, Höglund L, Ågren J (1992) On the numerical treatment of moving boundary problems. Z Metall 83:673–669
8. Elliott CM, Garcke H (1996) On the Cahn–Hilliard equation with degenerate mobility. SIAM J Math Anal 27:404–423
9. Elliott CM, Garcke H (1997) Diffusional phase transitions in multi-component systems with a concentration dependent mobility matrix. Physica D 109:242–256
10. Fan J, Han T, Haataja M (2010) Hydrodynamic effects on spinodal decomposition kinetics in planar lipid bilayer membranes. J Chem Phys 133(23): art no 235101
11. Garcke H (2003) On Cahn–Hilliard Systems with elasticity. Proc R Soc Edinb 133A:307–331
12. Garcke H, Niethammer B, Rumpf M, Weikard U (2003) Transient coarsening behaviour in the Cahn–Hilliard model. Acta Mater 51:2823–2830
13. Gefen A (2007) Risk factors for a pressure-related deep tissue injury: a theoretical model. Med Biol Eng Comput 45(6):563–573
14. Javierre E, Vuik C, Vermolen FJ, van der Zwaag S (2006) A comparison of numerical models for one-dimensional Stefan problems. J Comput Appl Math 192(2):445–459
15. Javierre E, Vuik C, Vermolen FJ, Segal A (2007) A level set method for a multidimensional vector Stefan problems:

dissolution of stoichiometric particles in multi-component alloys. J Comput Phys 224:222–240
16. Kim J (2005) A diffuse-interface model for axi-symmetric immiscible two-phase flow. Appl Math Comput 160:589–606
17. Kuhn A, Keller T, Lawrence M, Morari M (2009) A model for transcutaneous current stimulation: simulations and experiments. Med Biol Eng Comput 47(3): 279–289
18. Küpper T, Masbaum N (1994) Simulation of particle growth and Oswald ripening via the Cahn–Hilliard equation. Acta Metall Mater 42(6):1847–1858
19. Lowengrub J, Truskinovski L (1998) Quasi-incompressible Cahn–Hilliard fluids and topological transitions. Proc R Soc Lond A. 454:2617–2654
20. Macklin P, Lowengrub J (2007) Nonlinear simulation of the effect of microenvironment on tumor growth. J Theor Biol 245:677–704
21. Mauri R, Shinnar R, Triantafyllou G (1996) Spinodal decomposition in binary mixtures. Phys Rev E 53(3):2613–2623
22. Murray WD, Landis F (1959) Numerical and machine solutions of transient heat conduction problems involving freezing and melting. Trans ASME (C) J Heat Transf 245:106–112
23. Myhr OR, Grong Ø (2000) Modeling of non-isothermal transformations in alloys containing a particle distribution. Acta Mater 48(7):1605–1615
24. Natali AN, Forestiero A, Carniel EL, Pavan PG, Dal Zovo C (2010) Investigation of foot plantar pressure: experimental and numerical analysis. Med Biol Eng Comput 48(12):1167–1174
25. Niehammer B, Pego RL (1999) Non-self-similar behavior in the LSW theory of Ostwald ripening. J Stat Phys 95(5–6):867–902
26. Olofsson S-O, Boström P, Lagerstedt J, Andersson L, Adiels M, Perman J, Rutberg M, Li L, Borén J (2009) The lipid droplet: a dynamic prganelle, not only involved in the storage and turnover of lipids. In: Ehnholm C (ed) Cellular lipid metabolism. Springer, Berlin, New York, pp 1–26
27. Or-Tzadikario S, Sopher R, Gefen A (2010) Quantitative monitoring of lipid accumulation over time in cultured adipocytes as function of culture conditions: toward controlled adipose tissue engineering. Tissue Eng C 16:1167–1181
28. Osher S, Sethian JA (1988) Fronts propagating with curvature-dependent speed. J Comput Phys 141:12–49
29. Pego RL (1989) Front migration in the nonlinear Cahn–Hilliard equation. Proc R Soc Lond A 422:261–278
30. Portnoy S, Vuillerme N, Payan Y, Gefen A (2011) Clinically oriented real-time monitoring of the individual's risk for deep tissue injury. Med Biol Eng Comput 49(4):473–484
31. Segal A, Vuik C, Vermolen FJ (1998) A conserving discretization for the free boundary in a two-dimensional Stefan problem. J Comput Phys 141:1–21
32. Seitz PC, Reif M, Yoshikawa K, Jordan R, Tanaka M (2011) Dissipative structure formation in lipid/lipopolymer monolayers. J Phys Chem B 115(10):2256–2263
33. Temam R (1997) Infinite dimensional dynamical systems in mechanics and physics, 2nd ed. (Applied mathematical sciences, vol 68). Springer , New York
34. Ubachs RLJM, Schreurs PJG, Geers MGD (2004) A nonlocal diffuse interface model for microstructural evolution of tin–lead solder. J Mech Phys Solids 52:1763–1792
35. Vermolen FJ, Gholami-Gharashoo M, Zitha PLJ, Bruining J (2010) Numerical solutions of some diffuse interface problems: the Cahn–Hilliard equation and the model of Thomas and Windle. Int J Multiscale Comput Eng 7(6):523–543
36. Verschueren M (1999) A diffuse-interface model for structure development in flow. PhD Thesis, Eindhoven University of Technology, Eindhoven
37. Wise SM, Lowengrub JS, Friboes HB, Cristini V (2007) Three-dimensional multispecies nonlinear tumor growth-1: model and numerical method. J Theor Biol 253:524–543